Genetic Manipulation of FBP1 Expression in Breast Cancer Cells Reveals the Potential of FBP1 to Disrupt The Warburg Effect, and Nutrient Mediated Adaptive Post-Translational Regulation of FBP1 Protein Levels.

Ali Ghanem
Heidelberg University
Boilinh Troung
Heidelberg University
Stefan Wölfl (wolfl@uni-hd.de)
Institute of Pharmacy and Molecular Biotechnology, Heidelberg University https://orcid.org/0000-0002-9977-174X

Research

Keywords: gluconeogenic, metabolic, suppressor, cancers, breast tumours

Posted Date: November 16th, 2021

DOI: https://doi.org/10.21203/rs.3.rs-1030616/v1

Abstract

The key gluconeogenic enzyme Fructose 1,6 bisphosphatase has emerged as a potential metabolic tumour suppressor in recent years. Ablation of FBP1 expression in various tumours fosters metabolic rewiring towards an increased reliance on aerobic glycolysis. While FBP1 is completely repressed in many cancers, breast tumours display distinct FBP1 expression based on their subtype, hence making breast cancer a suitable model for discerning the effects of FBP1 in contexts of cancer initiation and progression. We used ectopic over-expression and CRISPR-Cas9 disruption to establish cell lineages with stable alterations in their FBP1 levels. Complete knock-outs of FBP1 on gene level confirm the major impact of FBP1 on cancer cell metabolism and proliferation. Moreover, our results reveal cancer subtype-specific peculiarities in response to ectopic FBP1 expression including a clear demonstration of an adaptive proteasomal degradation of FBP1 in breast cancer cells, which is regulated by glucose and nutrient availability. In addition to validating the suggested tumour suppressor role of FBP1, our findings demonstrate an efficient adaptive complex regulation of FBP1 expression and its impact on the adaptation of cancer cells to nutrient conditions. Our results highlight the importance of FBP1 ablation on the protein level and its potential relevance to cancer and beyond.

Summary/ Highlights

- FBP1 is a quasi-tumor suppressor, whose levels diminish with cancer initiation and/or progression.
- FBP1 expression inhibits glucose uptake and metabolism and promotes respiration and mitochondrial activity.
- The loss of FBP1 fosters the Warburg effect.
- We describe an additional layer of FBP1 depletion on the post translational level.
- Cells with diminished FBP1 use the proteasome system to degrade the FBP1 protein; this is reversible and happens only in the presence of glucose.
- This mechanism is reminiscent of the FBP1 regulation in yeast, required for rapid adjustment to nutrient availability and growth conditions.
- The glucose-mediated proteasomal degradation of FBP1 allows a self-propagating cycle of increased glucose uptake leading to further repression of FBP1, which in turn allows for increased glucose uptake.
- Consistently, higher levels of FBP1 correlated with broad inhibition of cell cycle factors especially belonging to the G2/M phase.

Introduction

Recent years have seen a surge in research exploring the relevance of gluconeogenesis and the key enzyme fructose-1,6-bis-phosphatase FBP1 in cancer contexts [1–5]. The epigenetic silencing of FBP1 has been observed in several types of tumours and linked to poorer prognoses [2, 3, 5–9]. For many cancers, the loss of FBP1 has been described as an advantageous event in the metabolic rewiring

towards aerobic glycolysis. However, some cancer types show ambivalence in their FBP1 expression, with FBP1 expression maintained in less critical lesions and FBP1-loss having a poor prognostic relevance[2]. Breast tumours with better survival rates show positive FBP1 expression, while the more advanced forms of basal-like, triple-negative and metastatic breast cancer lack FBP1 expression. [9, 10].

This heterogeneity of breast cancers in regard to FBP1 expression makes breast cancer cells an apt model to further investigate the effects and regulation of FBP1 in contexts of cancer. To address this issue, we established stable over-expressions and a CRISPR-Cas9 knock-out of FBP1 in cultured breast cancer cell lines representing the two major subtypes; luminal (MCF-7) and basal-like (MDA-MB-231) (Fig S1) to investigate the impact of FBP1 in breast cancer with emphasis on the particularities of the two cellular environments. This was achieved by characterising the proliferative, metabolic, and oxidative effects of stable FBP1 over-expression and knock-out.

We demonstrate evidence of non-genomic FBP1-repression promoting further metabolic reprogramming to foster the Warburg effect, including increased aerobic fermentation, and glucose catabolism through both the glycolytic and pentose phosphate pathways, in addition to an increase in the levels of particular amino acids derived from both pathways.

Our findings signify clear distinctions between the two cell types in their reaction to ectopic FBP1. Our findings demonstrate an important role for post-translational regulation of FBP1 levels in breast cancer cells by protein degradation, and the modulation of FBP1 levels based on nutrient availability in the medium.

The emergence of CRSPR-Cas9 as a highly malleable and adaptable tool has made precise gene editing more feasible than ever before [11, 12], and opened the avenue for new genetic screens and precise genomic target validation and confirmation of findings based on non-genomic interference studies (i.e. siRNA) [12–14]. Using CRISPR-Cas9 mediated gene knock out to generate a genomic deletion of FBP1 in cancer cells we observed some clear differences to all previous studies using shRNA or siRNA mediated knock-downs [1–5]. The results obtained further demonstrate the essential role of FBP1 in metabolic adjustment and confirm the role of FBP1 as an emerging tumour suppressor, and emphasize FBP1's potential to suppress cancer specific glycolysis driven metabolism.

Results

The ectopic expression of FBP1 slows down MCF-7 proliferation in presence of abundant glucose

Previous reports indicated an anti-proliferative effect of FBP1 in various cancer types [1–3, 5–7]. To assess the effect of FBP1 on proliferation, we used the protein-based SRB viability assay to assess the growth rate of stable MCF-7 lineages, in which we established various contexts of FBP1 (Fig S1). Cells with FBP1 over-expression exhibited slower growth than the vector control cells (Fig. 1a). Consistently,

knocking out FBP1 increased the growth rate of MCF-7 cells with stable CRISPR-Cas9 deletion compared to the unmodified wild type cells (Fig. 1a). The changes in growth rates were not reflected in the colony formation assay (Fig. 1c). This last finding indicates that FBP1 does not hamper tumorigenesis in this luminal breast cancer subtype, consistent with the positive FBP1 expression in primary and luminal breast cancers [2].

FBP1 is essential for glucose autotrophy in MCF-7 cells

Our previous work on yeast established that FBP1 is indispensible for a continued gluconeogenesis flux [15, 16]. We therefore assessed the proliferation and survival of FBP1-KO cells under glucose depletion. Glucose withdrawal specifically impacted FBP1-KO growth and survival while the wild-type cells continued proliferating. Complete glucose deprivation inhibited the proliferation of FBP1 KO cells starting at 3 days after glucose withdrawal (Fig. 1b). Consistently, limiting glucose in medium to 2mM had comparable effects on FBP1-KO. On the contrary, neither diminished glucose nor complete glucose deprivation affected the proliferation of the wild type MCF-7 cells (Fig. 1b). This result highlights both the indispensability of FBP1 activity for gluconeogenesis in MCF-7, and also ensures that FBP1 is the only isozyme in these cells capable of catalysing the dephosphorylation of F1,6bP.

FBP1 inhibits glucose uptake under a variety of conditions in MCF-7 cells

To test the impact of FBP1 on glucose uptake in MCF-7 cells, we used 2-NBDG (fluorescence labelled 2-DG). The over-expression of FBP1 inhibited glucose uptake in full DMEM, meanwhile FBP1 KO showed a general trend towards increased glycolysis (Fig. 2a). FBP1 over-expression also inhibited glucose uptake upon glucose replenishment and under glutamine deprivation (Fig. 2b)., consistent with the reports on the anti-glycolytic effect of FBP1 in various types of cancer [2–8].

FBP1 loss increases glucose utilisation in glycolysis, pentose phosphate pathway and amino acid synthesis

In line with earlier reports on FBP1 repression as an essential step towards Warburg metabolic rewiring [2, 3, 5], we used HPLC-MS metabolite quantification to investigate the metabolic shifts in FBP1 KO MCF-7 cells in contrast with the parental wild-type cells. FBP1 KO cells demonstrated an increased abundance of glycolysis and pentose phosphate pathway intermediates (Fig. 2c,d). Increased intracellular and extracellular lactate also indicates an increased glycolytic flux. Unlike the other glycolytic intermediates, phosphoenolpyruvate and pyruvate were both depleted in the FBP1 KO cells. The increase of the intracellular and extracellular lactate on expense of pyruvate is a clear sign of increased aerobic fermentation in the absence of FBP1 (Fig. 2c,g). Since pyruvate the most net consumed metabolite by cells (Fig S2), the depletion of pyruvate in medium and the increase in intracellular and medium lactate strongly signifies an overall increase in pyruvate conversion to lactate fuelled by both glycolytic and extracellular pyruvate. Altogether this indicates glucose to lactate metabolic flux, hence a potentiated Warburg effect in the FBP1 KO cells. The depletion of pyruvate and phosphoenolpyruvate in FBP1 KO

MCF-7 also coincided with an increase in alanine levels in medium, for which pyruvate is the biosynthetic precursor. Glutamine is the major nitrogen source and amino-acid in DMEM, with 2-D cultured cells showing higher reliance on glutamine compared to spheroids or in-vivo tumours [17]. The increased level of medium glutamine, observed for the MCF-7 KO cells (Fig. 2g), signifies a shift from amino acid to glucose catabolism upon FBP1 loss. Consistently, the overall output of extracellular alanine, which is net released from the cells into the medium (Fig S2), is increased, hence signifying an increased overall amino acid biosynthesis. Moreover, leucine, isoleucine, valine, tyrosine, tryptophan and phenylalanine, all essential amino acids, showed elevated accumulation in FBP1 KO cells hence indicating increased uptake and/or decreased catabolism due to the complete inhibition of gluconeogenesis (Fig S2).

A combination of GAPDH inhibition and of PKM2 activation causes serine depletion in FBP1 KO MCF-7

Intriguingly, and contrary to earlier findings [2], FBP1 KO correlated to a significant depletion of intracellular serine and its downstream derivative glycine (Fig. 2f). This depletion was not accompanied by shifts of either serine or glycine medium concentrations hence ruling out changes of uptake or secretion (Fig S2), while the activity of PHGDH, the key enzyme for serine biosynthesis [18], remained unchanged (Fig S3). Changes in glycolytic enzymatic activity offer a plausible explanation for the unexpected depletion of serine in FBP1 KO cells. We detected inhibited GAPDH activity and increased pyruvate kinase activity in the native protein extracts of the FBP1 KO cells compared to wild type (Fig S3). GAPDH inhibition is a reported mechanism of fuelling the pentose phosphate shunt with G6P [19–21], and it consists with the observed increase of upper glycolytic (Fig. 2c), and pentose phosphate pathway intermediates (Fig. 2d). FBP1 substrate F1,6bP is a robustly established allosteric activator of PKM2 [22, 23], hence the removal of FBP1 spares its substrate allowing the observed activation of PKM2. Together, inhibited GAPDH and activated PKM2 deplete the glycolytic intermediates in between the two enzyme, including 3-PG, the initial substrate of serine biosynthesis (Fig. 2c&f).

FBP1 impedes glucose sensing and uptake and in MCF-7 cells

To further assess the impact of FBP1 on glucose sensing, we probed TXNIP expression. TXNIP expression is indirectly induced by the glycolytic intermediates Glucose-6-phosphate G6P and glyceraldehyde-3phosphate GA3P [24]. Hence TXNIP is completely depleted under glucose deprivation. Under continuous glucose supply, and upon glucose replenishment, FBP1 KO cells exhibited higher levels of TXNIP compared to wild type cells (Fig. 3a,b&c). Consistently, lower levels of TXNIP expression were observed in FBP1 KO cells upon glucose replenishment with varying concentrations (Fig. 3d). To show that increased TXNIP expression is a direct outcome of increased glycolysis intermediates, 2-DG was included as a positive control and elicited sharp increase in TXNIP expression (Fig. 3d).

FBP1 correlates with increased ROS accumulation, mitochondrial biomass and decreased mitochondrial inner-membrane potential MIMP

In light of the observed effects on glucose catabolism and utilisation, we sought to assess the impact of FBP1 on the abundance and function of the mitochondria in addition to the related outcome of ROS accumulation. FACS analysis of DHE stained MCF-7 cells showed increased ROS accumulation in oeFBP1 vs vector control cells; consistently FBP1 KO cells exhibited significantly decreased ROS accumulation (Fig. 4a). Using MitoTracker® Green we similarly established a positive correlation between FBP1 expression and mitochondrial biomass (Fig. 4b), indicative of increased mitochondrial biogenesis in presence of FBP1. However, the increase in mitochondrial biomass with FBP1 expression also coincided with a diminished mitochondrial inner-membrane potential MIMP (Fig. 4c).

In line with the metabolic shift towards increased glucose catabolism and decreased glutamine consumption, we predicted that FBP1 loss would render cells independent of glutamine and more vulnerable to glucose starvation. Indeed, FBP1 absence prevented the additional ROS induction observed in glutamine deprived wild type cells (Fig. 4d), meanwhile the FBP1 KO cells responded to glucose withdrawal by dramatically increasing their mitochondrial biomass to levels significantly higher than the wild type (Fig. 4e). Therefore, suggesting a compensatory response to cope with glucose scarcity by increasing mitochondrial biomass to harness higher levels of energy form a dwindling level of metabolic intermediates.

The increase in mitochondria with lower MIMP can explain the elevated ROS as result of a concomitant increase in the overall mitochondrial inner-membrane area, as a result of increased mitochondrial biomass, and leakiness in the electron transport chain. This also consists with the FBP1 inhibitory effects on mitophagy, since electron transport chain leaking is a hallmark of aging mitochondria.

FBP1 deletion diverts ATP production from the ETC

Blocking ATP-synthase with 10μM oligomycin [25] resulted in significantly smaller increase of mitochondrial polarisation in FBP1 KO MCF-7 cells compared to the wild type (Fig. 4f). The increased polarisation reflects directly the amount of protons that would path through ATP-synthase and contribute to ATP production; hence we conclude that FBP1-deficinecy limited the reliance of MCF-7 on the electron transport chain ETC for ATP production.

This consists with the increased glucose consumption, utilisation and aerobic fermentation observed in the FBP1-KO cells.

FBP1-loss provides a survival advantage under extreme hypoxia

The increased glucose utilisation and aerobic fermentation we observed for FBP1 KO cells consist with the conventional Warburg effect, and should coincide with decreased reliance on respiration. Hence we investigated the survival of MCF-7 FBP1-KO cells under hypoxia compared to wild type cells. Both SRB growth/survival assay (Fig. 5a&b) and FACS analysis of PI-stained cells (Fig. 5c) showed a statistically valid advantage for FBP1-deficeint MCF-7 cells over the wild type cells following incubations at 1% O2 saturation, SRB assays were for a time frame of 24h to 96h under hypoxia, while PI staining was performed following 48h under 1% O2 saturation.

MDA-MB-231 cells acquire the capacity to degrade ectopic FBP1 in a proteasome dependent mechanism upon long-term selection

To better understand the metabolic and proliferative advantages of FBP1 silencing, we aimed to determine the effects of ectopic FBP1 in the triple-negative MDA-MB-231 cells, with depleted FBP1 expression. To our surprise the stable expression of FBP1, following a minimum of 6 weeks of geneticin selection, yielded diminished levels of FBP1 expression compared to the FBP1-positive MCF-7 (Fig. 6a). This was despite transient expression in MDA-MB-231 successfully yielding substantial levels of expression (Fig. 6b). Quantitative PCR also showed an increase in *FBP1* mRNA levels in MDA-MB-231 stable oeFBP1 cells, greater than that observed in MCF-7 oeFBP1 (Fig. 6c).

Altogether this indicated the potential of post-translational protein degradation as an underlying mechanism of the attenuated FBP1 expression in MDA-MB-231 cells.

To test this possibility we resorted to pharmacological proteasome inhibition [26]. Indeed, bortezomib treatment rescued FBP1 protein expression in MDA-MB-231 cells with stable FBP1 ectopic expression while showing no effect on FBP1 in the control MDA-MB-231 cells harbouring the empty vector (Fig. 6d). To verify the rescuing effect of proteasome inhibition on ectopic FBP1 expression in MDA-MB-231 cells we also used MG132, another more distinctive proteasome inhibitor [27], with comparable outcome to that observed with bortezomib (Fig. 6e). We are the first to observe such degradation of FBP1 in breast cancer cells, a similar effect has been found to contribute to FBP1 ablation in hepatocellular carcinoma [28].

Upon bortezomib treatment, the rescued ectopic FBP1 expression also inhibited glucose uptake compared to the vector control cells (Fig. 6f), similar to its identified role in MCF-7. Moreover, the transient transfection with FBP1, correlated to higher levels of expression, decreased acidification rates in MDA-MB-231 cells indicting slowed down glycolysis (Fig S4).

Glutamine as an exclusive carbon source stabilizes ectopic FBP1 expression in MDA-MB-231 cells and confreres a

growth disadvantage to oeFBP1 cells

We next sought to assess the interplay between the ectopic FBP1 expression in MDA-MB-231 and nutrient availability in the culture medium. The post-translational proteasome-dependent degradation of FBP1 has long been described as a part of the more encompassing phenomenon of carbon catabolite inactivation in unicellular eukaryotes [29]. Glucose is the most prominent metabolite to trigger the signalling cascade, which leads to FBP1 phosphorylation, ubiquitination, and degradation both in the proteasome and the vacuole [30, 31]. Therefore, we asked whether this mechanism is conserved in human cells. If so, the constitution and balance of carbon sources in cell culture medium should influence the observed levels of ectopic FBP1 by altering its degradation rate.

First, we observed via proliferation SRB assays that the marginal amounts of stably expressed FBP1 in MDA-MB-231 were advantageous under full DMEM containing both glucose and glutamine (Fig. 7a), as well as under high glucose concentration (75mM) with NH_4Cl as the exclusive nitrogen source (Fig. 7b), the successful utilisation of ammonia by breast cancer cells has been clearly demonstrated [32]. To our surprise however, the growth of oeFBP1 MDA-MB-231 cells was severely challenged in medium with high levels of glutamine (8mM) as the exclusive carbon and nitrogen source (Fig. 7c). This is very intriguing in light of glutamine being a major gluconeogenic substrate. Consistently, immunoblotting showed remarkable increase in ectopic FBP1 levels under glucose depletion coupled with high glutamine concentrations (Fig. 7d), thus indicating an attenuation of FBP1 degradation under this condition.

This is to our knowledge the first reported evidence on the effect of the availability of various carbon sources on FBP1 proteasomal degradation in human cancerous cells and mammalian cells in general. Hence indicating a likely carbon catabolite inactivation phenomenon akin to that characterised in yeast.

Despite its advantageous effect on proliferation, the presence of marginal ectopic FBP1 in oeFBP1 cells tangibly inhibited colony formation capacity (Fig. 7e), consistent with the known aspects of FBP1 repression in basal-like and metastasising breast cancer.

Stable and transient FBP1 expression lead to contrasting oxidative and mitochondrial outcomes in MDA-MB-231 cells

Compared to its effect in MCF-7, the stable expression of FBP1 in MDA-MB-231 unexpectedly correlated to a steep decrease in ROS levels as measured using DHE (Fig S5a). However, transient expression yielding comparable levels of FBP1 to those of MCF-7 had no significant effect on ROS accumulation (Fig S5d), despite a slight trend towards increased ROS. The investigated mitochondrial markers, on the other hand, reacted similarly to the expression of FBP1 in MDA-MB-231 in a manner comparable to the observations in MCF-7. MDA-MB-231 cells with stable FBP1 expression exhibited lower mitochondrial inner-membrane polarisation and higher total mitochondrial biomass (Fig S5b&c).

Transient FBP1 over-expression however yielded elevated mitochondrial polarisation (Fig S5e), hence possibly indicating an increase in respiratory activity upon FBP1 ectopic expression later followed by increased mitochondrial biogenesis.

Comparing transcriptional profiles signified a wide-scale cell-cycle inhibitory effect of long term FBP1 expression in MDA-MB-231 cells

Having observed that MDA-MB-231 cells adapt to FBP1 long-term expression by degrading FBP1 in the proteasome, we were intrigued to assess the shifts in transcription that can indicate the types of alterations occurring as a result of ectopically expressing FBP1 in MDA-MB-231 cells. Therefore, we used the Illumina RNA microarray system for a full transcriptome scale quantification of gene-expression of stable oeFBP1 vs vector control MDA-MB-231 cells.

Following the basic quantification of fold changes in FBP1 over-expression *vs* vector control cells, we performed a wide analysis of the impact of FBP1 over-expression on gene-expression patterns in MDA-MB-231 including a larger pool of up-regulated (≥1.6 folds) and down-regulated (≤0.65 folds) genes (Figure S6). Using the STRING functional protein association network, two separate schemes of interaction networks between the proteins encoded by the up-regulated and down-regulated genes were made. Comparing the two interaction networks, the most noticeable difference is the clear arrangement of the down-regulated genes into an interaction-rich network (Fig S6a). At the centre of this network are proteins associated with the cell cycle progression; the vast majority are proteins essential for mitosis and cytokinesis (M-Phase) these include the centrosome proteins CENP- A,E,M,N, aurora kinase A AURK-A and its activator TPX, the kinesin family members KIFs 2C, 4A, 20A, 20B, 23 and the centrosomal protein CEP55. Besides M-phase proteins, several other genes encoding for essential cell-cycle proteins are also seen within the aforementioned interaction network. These include, the Cyclin A2 essential for the cell cycle progression G1/S and G2/M transitions through activating CDK1 (also among the down-regulated genes) and CDK2. Other down-regulated genes include the histone cluster 2 (H2AC and H2AA3) in addition to thymidilate synthetase essential for thymidine de-novo biosynthesis and the exonuclease 1 EXO1 essential for DNA-mismatch repair. In contrast with the heavy interactions observed between the down-regulated genes, the interactions among the up-regulated genes are scarce. Therefore no wider conclusions regarding the up-regulation of entire signalling pathways or cellular functions could be drawn.

Immunoblotting confirmed the FBP1-associated inhibition of CENP-E

In order to test the observed cell-cycle inhibition on a protein level, immunoblots of short-term transfected MDA-MB-231 cells were performed. HT-29 cells were also included to test the validity of our findings in other FBP1-deficeint cell lines of other tumor origins. Consistent with the transcriptional findings, the

ectopic expression of FBP1 correlated to diminished CENP-E levels in both tested cell lines (Fig. 8). This finding validates the functional relevance of the cell cycle inhibition seen in the transcriptional profiling.

Discussion

This work aimed at investigating FBP1 as an emerging tumour suppressor in the context of breast cancer using cell lines representing the luminal and basal-like major subtypes. We studied the effects of FBP1-loss by establishing CRISPR-Cas9 knock-out of FBP1 in MCF-7 cells and characterising the resulting knock-out cell population against the otherwise genetically-identical parental MCF-7 population. Hence we are the first to share evidence from a genomic knock-out of FBP1 in cancer cells to support the tumour suppressor role ascribed to FBP1, its anti-glycolytic metabolic activity, and FBP1 repression as an important step towards aerobic glycolysis and fermentation typical to the Warburg effect [1–8]. Nonetheless, several particularities were identified for each cell type in regards to their response to ectopic FBP1 expression.

While the additional FBP1 over-expression in MCF-7 presented a burden on growth and glucose utilisation, the endogenously FBP1-repressed MDA-MB-231 adapted to the long-term expression of FBP1 by post-translational degradation. This left a marginal amount of FBP1 upon selection of MDA-MB-231 with stable FBP1 expression. This minute amount of FBP1 expression had favourable effects for growth under glucose, and inhibited ROS accumulation. To the contrary, interventions to restore high levels of the ectopically expressed FBP1 by proteasomal inhibition or growing cells with glutamine as the restrictive carbon source, unmasked the anti-proliferative and glucose uptake inhibition associated to high levels of FBP1 as in MCF-7 cells. Similarly, the transient expression in MDA-MB-231 yielded higher levels of expression and associated to inhibition of cellular acidification, did not inhibit ROS accumulation, and exhibited comparable effects on mitochondrial variables to those observed with oeFBP1 in MCF-7. In line with earlier findings, FBP1-associated increase in mitochondrial biomass also correlated with diminished survival under hypoxia indicating increased reliance on respiration in contexts of FBP1 expression. A similar pro respiratory effect and enhanced mitochondrial activity is common to other interventions that disrupt glycolysis, as we reported very recently in regards to the effect of concentrated ascorbate on breast cancer cells [33]. Furthermore, respiratory effects of FBP1 is probably an outcome of interplay between its negative impact on glycolytic flux and its non-catalytic role as a negative co-regulator of HIF1-alpha, which has been thoroughly described in renal cancer [3]. The presence of an identical mechanism in breast cancer is highly plausible, especially that a non-catalytic role of FBP1 in preventing snail mediated EMT has already been described in breast cancer cells [2], which suggests the possibility of a non-catalytic protein-protein interaction allowing FBP1 to function as a co-regulator of gene expression. Consistent with earlier works on FBP1 in breast and renal cancers [2, 3, 34], we showed evidence of increased mitochondrial biomass and reliance on respiration for energy generation and survival. The links between FBP1 and mitochondrial homeostasis and function offer a potential mechanism for interventions to target tumour metabolism and abrogate the transition towards aerobic fermentation by fostering cellular respiration using FBP1 metabolite activation [35] and epigenetic interventions to prevent FBP1 repression in cancer cells and/or precancerous lesions [36]. Moreover, the

FBP1-associated increase in mitochondrial mass and the reported prolonged mitochondrial retention due to inhibited mitophagy both suggest potential relevance of FBP1 and gluconeogenesis to aging and longevity. It is widely accepted that cumulative damage to the mtDNA and respiratory chain majorly contribute to aging [37, 38]. Hence the effects of FBP1 and gluconeogenesis on the mitochondrial homeostasis of aging cells could be relevant to longevity [39]. This is relevant in light of the potential nutritional regulation of FBP1 expression, for which our preliminary results already show a promise for modulating FBP1 levels in cancer cell lines by altering nutrients availability. It did not escape our attention that the stabilisation of ectopic FBP1 under glucose restriction and glutamine abundance could constitute a hitherto unobserved form of carbon catabolite repression of FBP1 in mammalian cells, similar to the well-characterised phenomenon in yeast [18, 29].

Proposed mechanism of dynamic FBP1 regulation light of the glucose-mediated post-translational inactivation of FBP1. Based on our observations we speculate that epigenetic silencing of FBP1 in cancer cells is incomplete and not sufficient for the metabolic adjustment driving cancer metabolism. Thus, silencing of FBP1 is complemented by post-translational repression. Vice versa, glucose withdrawal allows for the restoration of FBP1 expression in a self-sustaining cycle: diminished glucose levels alleviate the proteasomal degradation and the increased FBP1 level further inhibits glucose uptake and glycolysis and therefore keeps the glucose-mediated FBP1 post-translational inactivation at bay.

Since we reached these findings in cell culture by applying extreme and physiologically irrelevant conditions of glucose deprivation it remains to be seen how this mechanism applies in-vivo both in cancer cells, precancerous lesions, and under normal physiology in normal cells.

With that said and considering the newly described relevance of FBP1 to transcriptional control, the above described mechanisms of FBP1 restoration could open a door for the metabolic rewiring of cancer cells diverting them away from the Warburg model and limiting aggressiveness. Uncovering the in-vivo physiology of FBP1 post-translational control would be very relevant to both cancer and metabolic disease since it would mean that dietary and nutritional intervention can contribute to the long term sustenance or ablation of FBP1 expression. Furthermore, the dynamic effect of nutrient availability on FBP1 expression in cancer cells makes space for speculation regarding a plausible mechanism of the robust anti-cancer effect attributed to metformin in wide population studies showing diminished cancer risk in type-II diabetics on metformin [40]. In this mechanism the glucose lowering effect of metformin, especially via blocking the hepatic gluconeogenesis [41], would have a stabilising effect on FBP1 expression in the periphery and preserve its quasi tumour suppressor role. We are therefore focused on further identifying the molecular mechanism, magnitude, and versatility of this effect.

Conclusions

In this study we provided the first genomic-based evidence on the relevance of FBP1 to the emergence of Warburg effect. We also demonstrated for the first time the capability of particular breast cancer cells to

degrade FBP1 as a response to its enforced ectopic expression. Moreover, we also analysed the effect of nutrient availability in the culture medium on FBP1 mediated effects on cellular proliferation and survival.

Our current and future work will focus on identifying the exact mechanism behind FBP1 post-translational regulation in cancer cells in the hope of identifying physiologically relevant mechanisms contributing to FBP1 ablation in cancer initiation and progression, in addition to metabolic diseases.

Methods

Cell culture: the cell-lines MCF-7, MDA-MB-231 (ATCC) were incubated at 37° and 5% CO2. All passaging, cultivation, seeding and treatments were performed in Dublecco's modified eagle medium DMEM (Gibco, Germany) for details refer to **Supp. Methods I**.

MCF-7 and MDA-MB-231 cells (ATCC) were obtained in 2012, preserved in liquid nitrogen and utilized for experiments in passage between 15 and 30. Cells were also tested for mycoplasma. Further details in **Supp. Methods I**.

Cells were treated with various media conditions as indicated, fresh DMEM was prepared from scratch with glucose, glutamine, and NH4Cl added freshly to reach the indicated concentrations. For proteasome inhibition, bortezomib (Selleckchem®) and MG132 (Sigma-Aldrich®) were used.

Molecular cloning and construction of plasmids

To establish ectopic expression of FBP1 in the tested cell lines, new plasmids were constructed with FBP1 variants expressed under a constitutive mammalian promoter. For this purpose I started with the commercially available pcDNA3.1(-) vector.

(For the detailed method please refer to the **Supp. Methods II**)

Transfection of cell lines and establishing stable over-expressions and deletions

Lipid-based transfection was used, Lipofectamin^{TM}3000 (Thermo Fisher®, Waltham MA), for introducing the FBP1 over-expression or CRISPR-Cas9 deletion vectors into the cell lines. The transfections were performed using the protocols provided with the transfection reagents.

(The detailed methods of trnasfection and establishing the stable cell lineages in the **Supp. Methods III**)

Protein extraction for immunoblotting

To extract total proteins from cells, $3*10^5$ to $5*10^5$ cells were seeded, following 24 to 48 hours of incubation cells were subjected to the desired treatment or medium conditions and then lysed in 6 M urea buffer containing the following protease inhibitors: (NaF, PMSF, Pepstatin, Aprotenine and $NaVO_4$). To lyse the cells, medium was aspirated, and 120 to 180 µl ice-cold 6 M Urea buffer were pipetted directly

onto the cells. Subsequently, the cell culture plates were promptly placed on ice and then vortexed to ensure full homogenization in the Urea buffer. Afterwards, lysates were collected in Eppendorf tubes and then spun down at 13000 g for 15 minutes to get rid of the DNA. Lysates were subsequently stored at -20°C.

Determining total protein concentrations

Total protein concentrations in the lysates were determined using Bradford reaction. 10 µl of each lysates were mixed with 990 µl of Bradford reagent (Sigma-Aldrich) in Eppendorf tubes. Samples were then mixed and incubated for 5 minutes in the dark. Subsequently 3x300 µl of each sample were transferred into 96 well-plates and measured using the Tecan Ultra (Tecan, Germany) reader at 595 nm.

SDS-PAGE and immunoblotting

Proteins in denatured lysates were resolved on 10% polyacrylamide gel (SDS-PAGE) as described in (Laemmli, 1970)[42]. Afterwards, resolved proteins were blotted (transferred) from the resolving SDS-PAGE gel onto a PVDF membrane. Semi-dry protein transfer was used with anode and cathode buffer prepared as detailed in the above material section.

Subsequently, membranes were stained with ponceau S (5% ponceau S) and then washed in TBS-tween 1% *(v/v)* buffer and blocked in a 5% BSA solution in TBS-tween buffer for 1 hour, and then incubated with 1:1000 solution of one of the used primary antibodies. After the primary anti-body incubation, membranes were washed 3 times for 5 minutes each in TBS-tween 1 buffer and subsequently incubated in 1:5000 HRP-fused anti rabbit or anti mouse secondary (IgG) anti-body solutions for 1 hour. Finally, membranes were washed 3 x 5 minutes and developed in Western Lightning Plus-ECL (Perkin-Elmer, Germany). Signals were detected using the Fujifilm LAS-3000 imaging system and the AIDA software for image acquisition.

Quantification of western-blot signals

the intensities of the western-blot bands of target proteins were quantified using the Image-J histogram quantification tool. The intensity of the target protein signals was adjusted relative to the corresponding loading-control (beta-actin) bands.

SRB Survival and growth assays

The total-protein based SRB colourimetric assay was used to assess cell survival and growth of cells with various FBP1 contexts under the indicated media conditions/treatments.

The utilised SRB-assay protocol was derived from Vichai and Kirtikara 2006 [43].

For the detailed SRB method refer to the **Supp. Methods IV**)

FACS analysis

Fluorescence activated cell sorting FACS analysis was used to measure a variety of metabolic and viability markers in the cells. Cells were seeded in 12 well plates at a density of 50,000 cells/well in 1 ml full DMEM/well and incubated over-night. On the following day medium was aspirated, and cells were treated as indicated for each experiment). Following treatment, cells were incubated with the fluorescent probes) then analysed using FACS Guava (Merck-Millipore, UK).

The following probes were used; 2-NBDG for glucose uptake[44], DHE for intracellular ROS accomulation [45], MitTracker Green for mitochondrial mass, and JC-1 for mitochondrial inner-membrane potential.

(Detailed methods and mechanisms for each fluorescent probe are listed in the **Supp. Methods V.)**

Liquid chromatography-mass spectrometry based metabolite quantification:

Intracellular metabolites were extracted and quantified using an LC-MS based method as previously described in [46]. Details in **Supp. Methods VI**.

Extraction of RNA from cultured cells

Cells were seeded in full DMEM in six-well plates at a density of $2x10^5$ cells/well. After 1 day cells were treated, or transfected as indicated, and after the indicated duration of treatment mRNA was extracted using the following triazole/chloroform method.

(For the detailed methods of the mRNA extraction refer to the **Supp. Methods VII**.)

Complementary DNA (cDNA) synthesis

The synthesis of cDNA from the isolated RNA was carried out using the ProtoScript® First Strand Synthesis kit from NEB®.

The cDNA was synthesised using the protocol provided with the kit. To ensure that the mRNA is exclusively reverse-trscribed without other RNA types in the mixture, the reverse transcription was performed using poly-t primers that anneal specifically to the poly-A tails of the mRNA transcripts.

Real-time quantitative PCR rt-qPCR

For the quantitative PCR the LightCycler® Sybr Green (Roche®) reaction mix was utilized. The reactions were prepared according to the following protocol:

The following master-mix was prepared for each primer pair (target gene) to be tested. Quantities are giver for 1 reaction:

- Cybr Green®: 2.5 µl
- Primer Mix: 1 µl
- Nuclease free water: 0.5 ml

Pipetted onto 1 µl of cDNA (concnetration≈30 ng/µl)

The tested cDNAs were pipetted in Microplate 96 LP (Analytik Jena AG) compatible to the qTOWER real-time PCR thermal cycler (Analytik Jena AG).

4 µl of the master-mix were pipetted in triplets on each type of the tested cDNAs. Subsequently, the plates were fed into the qTower real-time PCR thermal cycler, where the reactions occurred and the results were obtained.

Quantitative interpretation of the qPCR data

The mean values of the yielded CT of each triplet or reactions were calculated, including the mean-values of each tested cDNA with the reference genes. Then using these mean values of the CT of each target and reference genes, relative expression of the target genes was compared for the different cDNAs (treated vs non-treated or transfected vs empty vector) using the ΔΔCT equation to yield the relative expression values:

$\Delta Ct = Ct_{(target\ gene)} - Ct_{(reference\ gene)}$ for a given sample.

$\Delta\Delta Ct = \Delta Ct_{(treated\ sample)} - \Delta Ct(control\ sample)$

Relative expression (Fold change)$= -2^{\Delta\Delta Ct}$

Transcriptional profiling of MDA-MB-231 cells

RNA was extracted from 500.000 cells. RNA concentrations were adjusted to 100ng/µl and samples were sent to collaborators in the Functional Genome Analysis Division in DKFZ (Lab of Professor Jörg Hoheisel), were they were analysed using the Illumina RNA microarray system. The utilised method was described in previously published research from the group [47]and is summarised below:

- RNA-integrity of the samples was verified using Agilent 2100 Bioanalyzer (Agilent Technologies, Palo Alto).
- The analysis of the total RNA in the samples was performed using Sentrix Human-6v3 Whole Genome Expression BeadChips (Sentrix Human WG-6; Illumina).
- Following hybridisation to the chips according to the manufacturer's instructions, the arrays were scanned with a BeadArray Reader (Illumina).

Colony forming assay

Cells with different FBP1 expression were seeded in 6 well plates at the extra-low density of 300 cells/well in 2 ml full DMEM, refreshed every 7 days. After 2 weeks (MDA-MB-231) or 3 weeks (MCF-7) of incubation colonies were fixed and stained using a PBS solution containing 0.021% *(v/v)* formaldehyde and 0.5% *(w/v)* crystal violet.

Declarations

Competing interests

The authors declare no conflict of interests.

Authors' contributions

Concept and experimental design A.G. and S.W.; Experimentation; A.G. and B.T.; Methodology A.G. and S.W.; Funding and Supervision S.W.; Data analysis and interpretation A.G. and S.W.; Data presentation and figure design A.G. and S.W.; drafting the manuscript A.G. and S.W. All authors read and approved the manuscript before submission.

Funding

A.G. received a DAAD fellowship to pursue his PhD in the Wölfl Lab, parts of this study were also supported by BMBF funding with the following grants FKZ 01EK1612C and FKZ 031A303E. We would also like to acknowledge the financial support from the DFG and Heidelberg University within the Open Access Publishing.

Acknowledgements

We thank Esther Zaal and Celia Berkers (Utrecht University) for their support with the metabolite quantification using HPLC-MS in addition to Andrea Bauer and Jörg Hoheisel (DKFZ) for their support with preliminary transcriptional profiling.

Ethical approval and consent to participate and consent for publication

We conducted our study in standard breast cancer cell lines with no patient material or animals involved. Hence no ethical approval or consents were required.

Availability of data and material

All data and material connected to this work are available and can be provided upon request.

References

1. Chen M, Zhang J, Li N, Qian Z, Zhu M, Li Q, Zheng J, Wang X, Shi G: **Promoter hypermethylation mediated downregulation of FBP1 in human hepatocellular carcinoma and colon cancer**. *PLoS One* 2011, **6**(10):e25564.
2. Dong C, Yuan T, Wu Y, Wang Y, Fan TW, Miriyala S, Lin Y, Yao J, Shi J, Kang T *et al*: **Loss of FBP1 by Snail-mediated repression provides metabolic advantages in basal-like breast cancer**. *Cancer Cell* 2013, **23**(3):316–331.

3. Li B, Qiu B, Lee DS, Walton ZE, Ochocki JD, Mathew LK, Mancuso A, Gade TP, Keith B, Nissim I *et al*: **Fructose-1,6-bisphosphatase opposes renal carcinoma progression**. *Nature* 2014, **513**(7517):251–255.
4. Zhang J, Wang J, Xing H, Li Q, Zhao Q, Li J: **Down-regulation of FBP1 by ZEB1-mediated repression confers to growth and invasion in lung cancer cells**. *Mol Cell Biochem* 2016, **411**(1-2):331–340.
5. Zhu Y, Shi M, Chen H, Gu J, Zhang J, Shen B, Deng X, Xie J, Zhan X, Peng C: **NPM1 activates metabolic changes by inhibiting FBP1 while promoting the tumorigenicity of pancreatic cancer cells**. *Oncotarget* 2015, **6**(25):21443–21451.
6. Sheng H, Ying L, Zheng L, Zhang D, Zhu C, Wu J, Feng J, Su D: **Down Expression of FBP1 Is a Negative Prognostic Factor for Non-Small-Cell Lung Cancer**. *Cancer Invest* 2015, **33**(5):197–204.
7. Li J, Wang Y, Li QG, Xue JJ, Wang Z, Yuan X, Tong JD, Xu LC: **Downregulation of FBP1 Promotes Tumor Metastasis and Indicates Poor Prognosis in Gastric Cancer via Regulating Epithelial-Mesenchymal Transition**. *PLoS One* 2016, **11**(12):e0167857.
8. Hirata H, Sugimachi K, Komatsu H, Ueda M, Masuda T, Uchi R, Sakimura S, Nambara S, Saito T, Shinden Y *et al*: **Decreased Expression of Fructose-1,6-bisphosphatase Associates with Glucose Metabolism and Tumor Progression in Hepatocellular Carcinoma**. *Cancer Res* 2016, **76**(11):3265–3276.
9. Li H, Li M, Pang Y, Liu F, Sheng D, Cheng X: **Fructose1,6bisphosphatase1 decrease may promote carcinogenesis and chemoresistance in cervical cancer**. *Mol Med Rep* 2017, **16**(6):8563–8571.
10. Cheng P, Wang Z, Hu G, Huang Q, Han M, Huang J: **A prognostic 4-gene expression signature for patients with HER2-negative breast cancer receiving taxane and anthracycline-based chemotherapy**. *Oncotarget* 2017, **8**(61):103327–103339.
11. Wang H, La Russa M, Qi LS: **CRISPR/Cas9 in Genome Editing and Beyond**. *Annu Rev Biochem* 2016, **85**:227–264.
12. Doudna JA, Charpentier E: **Genome editing. The new frontier of genome engineering with CRISPR-Cas9**. *Science* 2014, **346**(6213):1258096.
13. Moore JD: **The impact of CRISPR-Cas9 on target identification and validation**. *Drug Discov Today* 2015, **20**(4):450–457.
14. Lu Q, Livi GP, Modha S, Yusa K, Macarron R, Dow DJ: **Applications of CRISPR genome editing technology in drug target identification and validation**. *Expert Opin Drug Discov* 2017, **12**(6):541–552.
15. Ghanem A, Kitanovic A, Holzwarth J, Wolfl S: **Mutational analysis of fructose-1,6-bis-phosphatase FBP1 indicates partially independent functions in gluconeogenesis and sensitivity to genotoxic stress**. *Microb Cell* 2017, **4**(2):52–63.
16. Kitanovic A, Wolfl S: **Fructose-1,6-bisphosphatase mediates cellular responses to DNA damage and aging in Saccharomyces cerevisiae**. *Mutat Res* 2006, **594**(1-2):135–147.
17. Muir A, Danai LV, Vander Heiden MG: **Microenvironmental regulation of cancer cell metabolism: implications for experimental design and translational studies**. *Dis Model Mech* 2018, **11**(8).

18. Hammerle M, Bauer J, Rose M, Szallies A, Thumm M, Dusterhus S, Mecke D, Entian KD, Wolf DH: **Proteins of newly isolated mutants and the amino-terminal proline are essential for ubiquitin-proteasome-catalyzed catabolite degradation of fructose-1,6-bisphosphatase of Saccharomyces cerevisiae**. *J Biol Chem* 1998, **273**(39):25000–25005.
19. Kuehne A, Emmert H, Soehle J, Winnefeld M, Fischer F, Wenck H, Gallinat S, Terstegen L, Lucius R, Hildebrand J *et al*: **Acute Activation of Oxidative Pentose Phosphate Pathway as First-Line Response to Oxidative Stress in Human Skin Cells**. *Mol Cell* 2015, **59**(3):359–371.
20. Ralser M, Wamelink MM, Kowald A, Gerisch B, Heeren G, Struys EA, Klipp E, Jakobs C, Breitenbach M, Lehrach H *et al*: **Dynamic rerouting of the carbohydrate flux is key to counteracting oxidative stress**. *J Biol* 2007, **6**(4):10.
21. Dick TP, Ralser M: **Metabolic Remodeling in Times of Stress: Who Shoots Faster than His Shadow?** *Mol Cell* 2015, **59**(4):519-521.
22. Dombrauckas JD, Santarsiero BD, Mesecar AD: **Structural basis for tumor pyruvate kinase M2 allosteric regulation and catalysis**. *Biochemistry* 2005, **44**(27):9417–9429.
23. Dayton TL, Jacks T, Vander Heiden MG: **PKM2, cancer metabolism, and the road ahead**. *EMBO Rep* 2016, **17**(12):1721–1730.
24. Wu N, Zheng B, Shaywitz A, Dagon Y, Tower C, Bellinger G, Shen CH, Wen J, Asara J, McGraw TE *et al*: **AMPK-dependent degradation of TXNIP upon energy stress leads to enhanced glucose uptake via GLUT1**. *Mol Cell* 2013, **49**(6):1167-1175.
25. Salomon AR, Voehringer DW, Herzenberg LA, Khosla C: **Understanding and exploiting the mechanistic basis for selectivity of polyketide inhibitors of F(0)F(1)-ATPase**. *Proc Natl Acad Sci U S A* 2000, **97**(26):14766–14771.
26. Buac D, Shen M, Schmitt S, Kona FR, Deshmukh R, Zhang Z, Neslund-Dudas C, Mitra B, Dou QP: **From bortezomib to other inhibitors of the proteasome and beyond**. *Curr Pharm Des* 2013, **19**(22):4025–4038.
27. Guo N, Peng Z: **MG132, a proteasome inhibitor, induces apoptosis in tumor cells**. *Asia Pac J Clin Oncol* 2013, **9**(1):6–11.
28. Jin X, Pan Y, Wang L, Zhang L, Ravichandran R, Potts PR, Jiang J, Wu H, Huang H: **MAGE-TRIM28 complex promotes the Warburg effect and hepatocellular carcinoma progression by targeting FBP1 for degradation**. *Oncogenesis* 2017, **6**(4):e312.
29. Chen SJ, Wu X, Wadas B, Oh JH, Varshavsky A: **An N-end rule pathway that recognizes proline and destroys gluconeogenic enzymes**. *Science* 2017, **355**(6323).
30. Schork SM, Bee G, Thumm M, Wolf DH: **Catabolite inactivation of fructose-1,6-bisphosphatase in yeast is mediated by the proteasome**. *FEBS Lett* 1994, **349**(2):270–274.
31. Horak J, Regelmann J, Wolf DH: **Two distinct proteolytic systems responsible for glucose-induced degradation of fructose-1,6-bisphosphatase and the Gal2p transporter in the yeast Saccharomyces cerevisiae share the same protein components of the glucose signaling pathway**. *J Biol Chem* 2002, **277**(10):8248–8254.

32. Spinelli JB, Yoon H, Ringel AE, Jeanfavre S, Clish CB, Haigis MC: **Metabolic recycling of ammonia via glutamate dehydrogenase supports breast cancer biomass**. *Science* 2017, **358**(6365):941–946.
33. Ghanem A, Melzer AM, Zaal E, Neises L, Baltissen D, Matar O, Glennemeier-Marke H, Almouhanna F, Theobald J, Abu El Maaty MA *et al*: **Ascorbate kills breast cancer cells by rewiring metabolism via redox imbalance and energy crisis**. *Free Radic Biol Med* 2021, **163**:196-209.
34. Shi L, He C, Li Z, Wang Z, Zhang Q: **FBP1 modulates cell metabolism of breast cancer cells by inhibiting the expression of HIF-1alpha**. *Neoplasma* 2017, **64**(4):535–542.
35. Icard P, Fournel L, Coquerel A, Gligorov J, Alifano M, Lincet H: **Citrate targets FBPase and constitutes an emerging novel approach for cancer therapy**. *Cancer Cell Int* 2018, **18**:175.
36. Yang J, Jin X, Yan Y, Shao Y, Pan Y, Roberts LR, Zhang J, Huang H, Jiang J: **Inhibiting histone deacetylases suppresses glucose metabolism and hepatocellular carcinoma growth by restoring FBP1 expression**. *Sci Rep* 2017, **7**:43864.
37. Sun N, Youle RJ, Finkel T: **The Mitochondrial Basis of Aging**. *Mol Cell* 2016, **61**(5):654–666.
38. Bratic A, Larsson NG: **The role of mitochondria in aging**. *J Clin Invest* 2013, **123**(3):951–957.
39. Liu Y, Jiang Y, Wang N, Jin Q, Ji F, Zhong C, Zhang Z, Yang J, Ye X, Chen T: **Invalidation of mitophagy by FBP1-mediated repression promotes apoptosis in breast cancer**. *Tumour Biol* 2017, **39**(6):1010428317708779.
40. Vancura A, Bu P, Bhagwat M, Zeng J, Vancurova I: **Metformin as an Anticancer Agent**. *Trends Pharmacol Sci* 2018, **39**(10):867–878.
41. Hunter RW, Hughey CC, Lantier L, Sundelin EI, Peggie M, Zeqiraj E, Sicheri F, Jessen N, Wasserman DH, Sakamoto K: **Metformin reduces liver glucose production by inhibition of fructose-1-6-bisphosphatase**. *Nat Med* 2018, **24**(9):1395-1406.
42. Laemmli UK: **Cleavage of structural proteins during the assembly of the head of bacteriophage T4**. *Nature* 1970, **227**(5259):680–685.
43. Vichai V, Kirtikara K: **Sulforhodamine B colorimetric assay for cytotoxicity screening**. *Nat Protoc* 2006, **1**(3):1112–1116.
44. Zou C, Wang Y, Shen Z: **2-NBDG as a fluorescent indicator for direct glucose uptake measurement**. *J Biochem Biophys Methods* 2005, **64**(3):207–215.
45. Zhao H, Kalivendi S, Zhang H, Joseph J, Nithipatikom K, Vasquez-Vivar J, Kalyanaraman B: **Superoxide reacts with hydroethidine but forms a fluorescent product that is distinctly different from ethidium: potential implications in intracellular fluorescence detection of superoxide**. *Free Radic Biol Med* 2003, **34**(11):1359–1368.
46. Zaal EA, Wu W, Jansen G, Zweegman S, Cloos J, Berkers CR: **Bortezomib resistance in multiple myeloma is associated with increased serine synthesis**. *Cancer Metab* 2017, **5**:7.
47. Bauer AS, Nazarov PV, Giese NA, Beghelli S, Heller A, Greenhalf W, Costello E, Muller A, Bier M, Strobel O *et al*: **Transcriptional variations in the wider peritumoral tissue environment of pancreatic cancer**. *Int J Cancer* 2018, **142**(5):1010–1021.

48. Perelman A, Wachtel C, Cohen M, Haupt S, Shapiro H, Tzur A: **JC-1: alternative excitation wavelengths facilitate mitochondrial membrane potential cytometry**. *Cell Death Dis* 2012, **3**:e430.

Scheme

Schemes 1 and 2 are available in the Supplemental Files section.

Figures

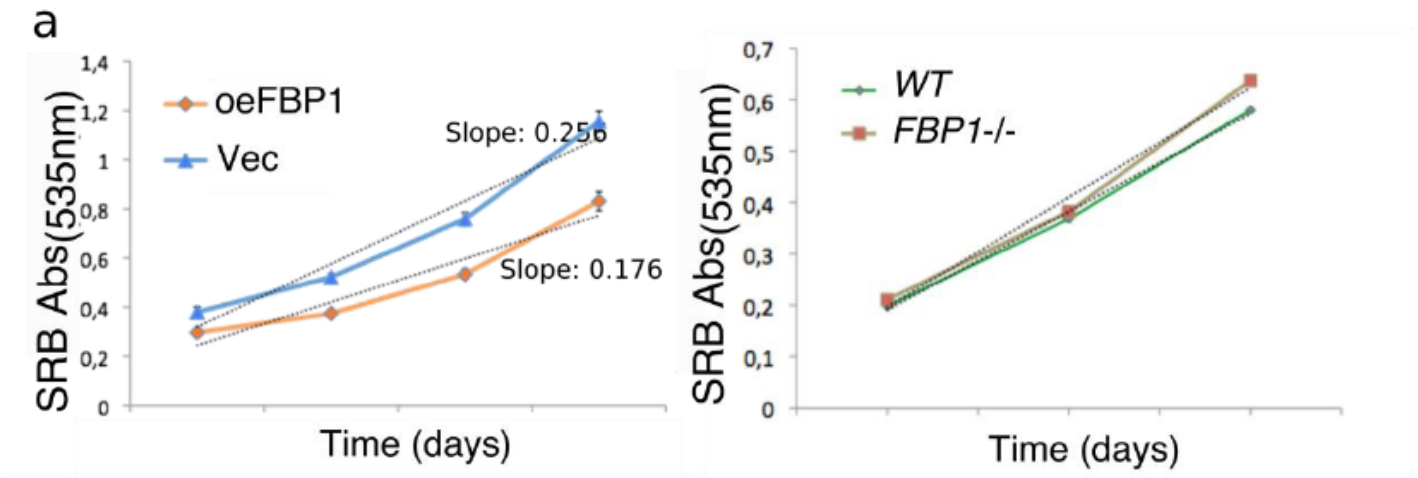

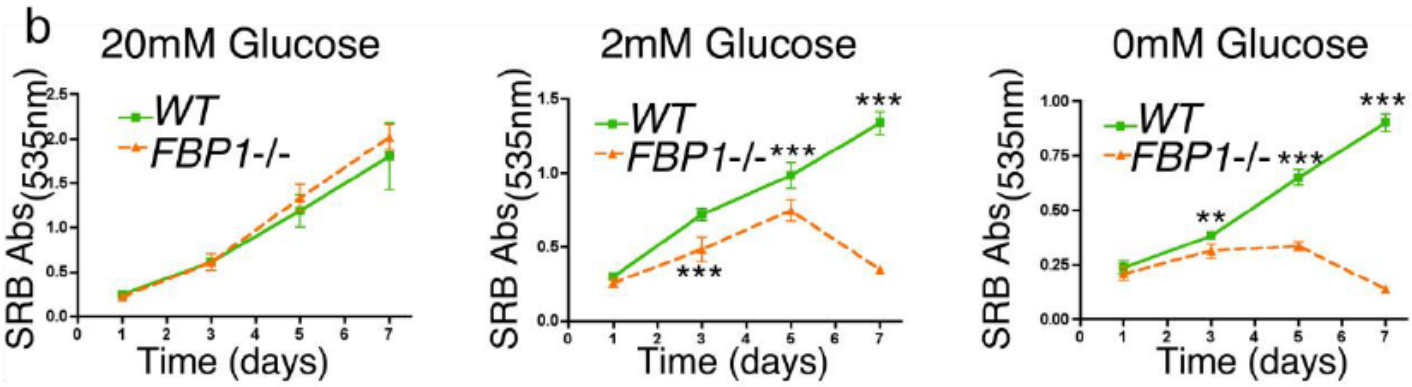

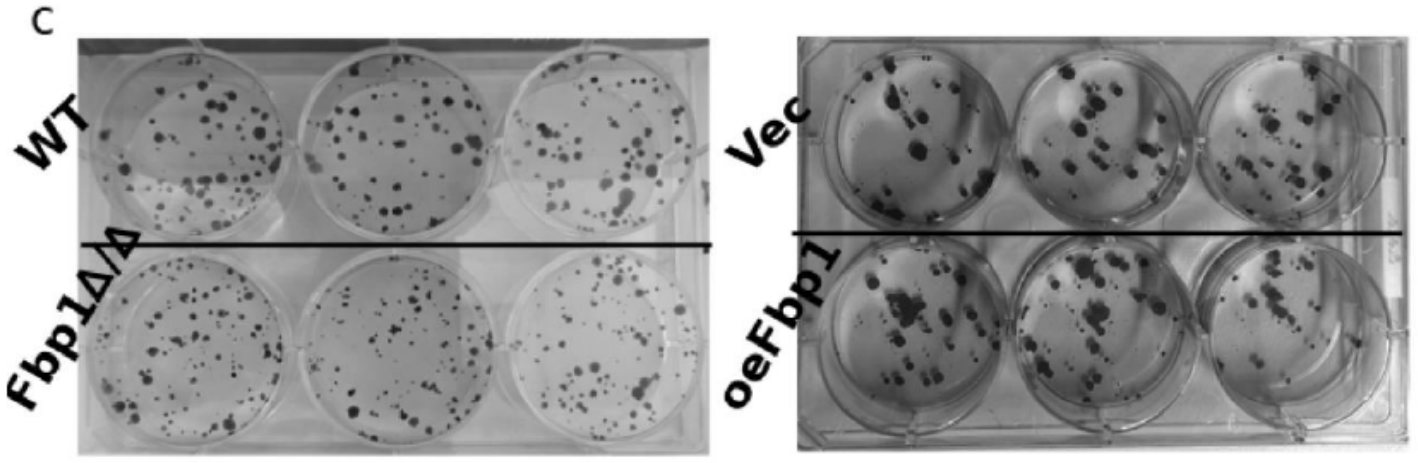

Figure 1

FBP1 effects on proliferation and colony formation of MCF-7 cells a) SRB proliferation assays of MCF-7 oeFBP1 vs vector control cells (left) and of the FBP1-/- vs wild-type (right). b) SRB proliferation assays of MCF-7 cells with DMEM medium containing various glucose concentrations (20mM, 2mM and 0mM). a&b) Data points show mean-values ±SD (n= 5 or 6). c) Colony formation assay of MCF-7 cells in full DMEM (3 weeks incubation in full DMEM, weekly replaced).

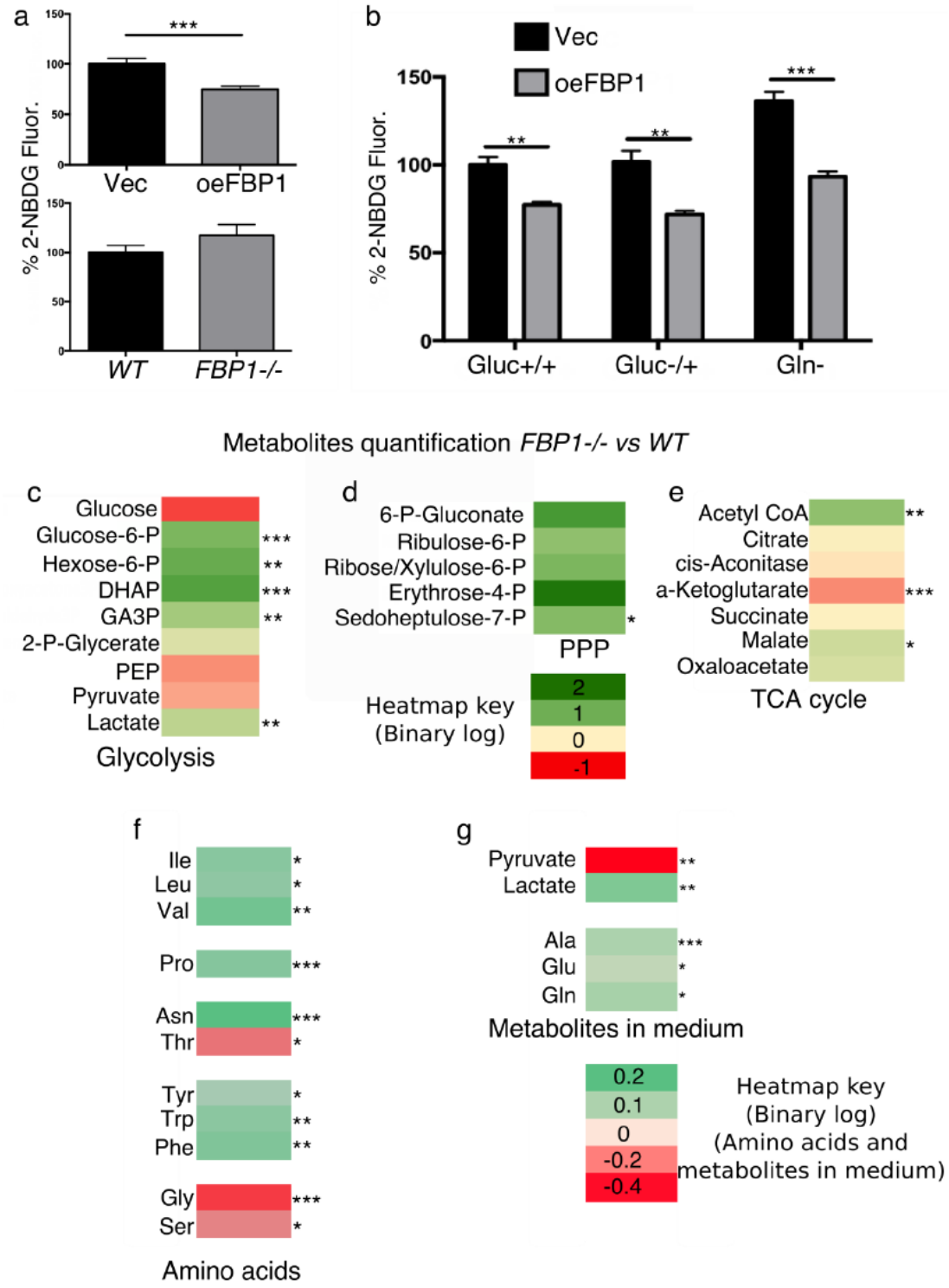

Figure 2

The over-expression of FBP1 slows down glucose uptake, while the deletion thereof induces glycolytic flux in MCF-7 cells. a) Glucose uptake in full DMEM (20mM glucose, 2mM glutamine) measured by FACS analysis of MCF-7 cells incubated with 2-NBDG for 4 hours. 5000 cells were analyzed; featured are the mean values ±SD (n≥4). b) Glucose uptake of MCF-7 cells in glutamine-depleted DMEM and following depletion and replenishment of Glucose. Glucose was withdrawn for 16 hours, followed by 4 hours of glucose replenishment at 20mM Glucose (Glu-/+) accompanied by 2-NBDG. Glutamine was withdrawn for a total of 20 hours (Gln-), including the last 4 hours of incubation with 2-NBDG. c to f) HPLC-MS quantification of intracellular metabolites in FBP1-/- MCF-7 cells relative to wild-type MCF7 cells; c) glycolytic intermediates, d) pentose phosphate pathway e) TCA cycle f) amino-acids exhibiting statistically significant shift in their abundance in FBP1 K.O vs wild type. g) Significantly altered extracellular metabolite abundances in the cell culture medium. The colours in the heat map indicate the relative abundance of the metabolites (in binary log) in FBP1 KO cells relative to the parental MCF-7 wild type population. Statistical significance is indicated with asterisks to the right.

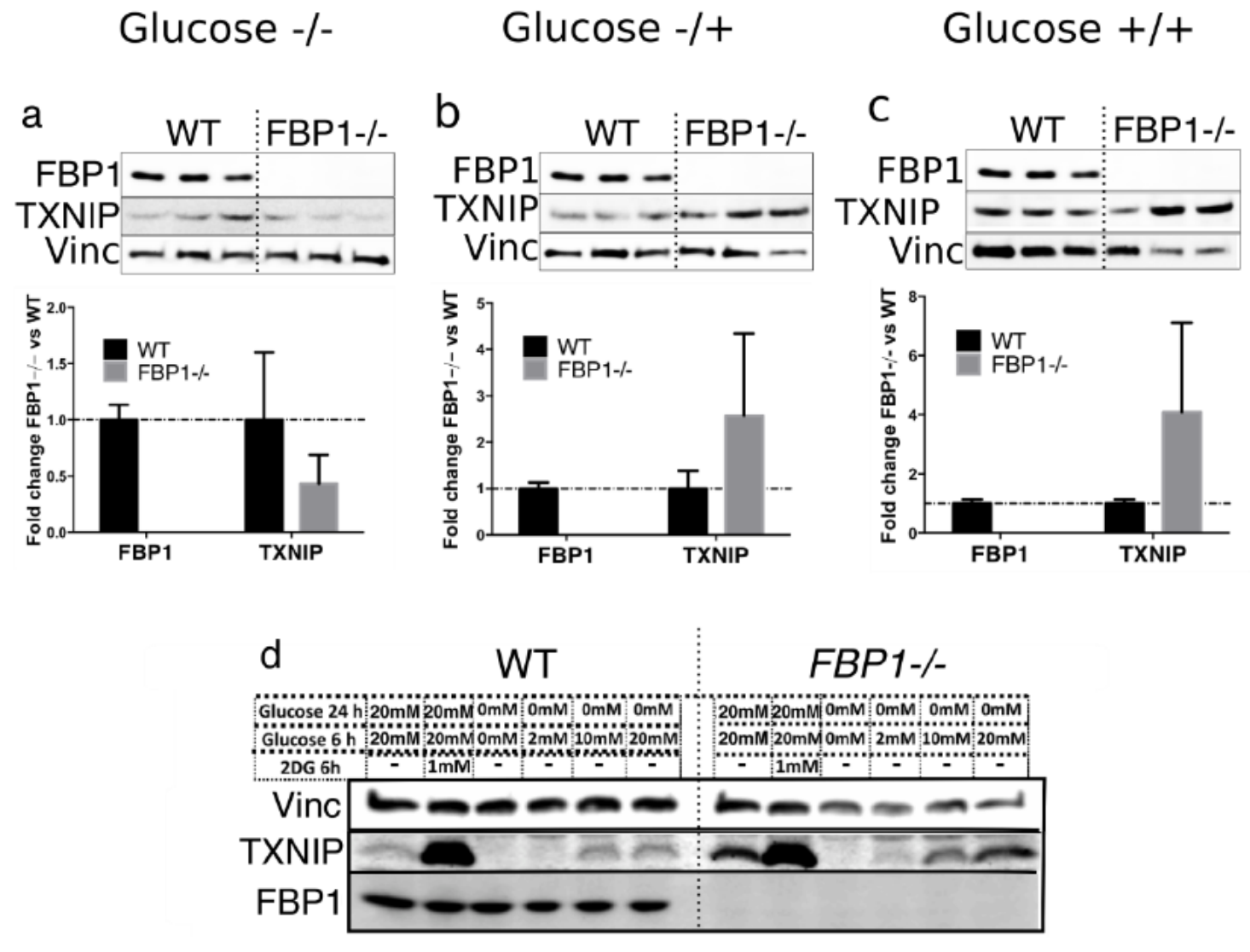

Figure 3

Western-blots showing the FBP1-related alterations in glucose sensitivity and response to glucose starvation in MCF-7 cells. a) Full glucose deprivation 0mM glucose for 24 hours. b) Glucose replenished condition; 20 hours of glucose starvation followed by 4 hours of glucose replenishment 20mM. c) Full medium 20mM glucose. All western-blots feature biologically independent, simultaneously treated triplets of wild type and FBP1-knockout MCF7. (The bar-blots below the western-blots in a, b and c indicate semi-quantification of the FBP1 and TXNIP signals normalized to the respective housekeeping signals. The featured values represent mean ±SD, n=3). d) The effects of various glucose starvation and replenishment conditions (as indicated in the charts above the blots) in addition to 2-DG as a positive control for glycolytic metabolite accomulation and TXNIP induction.

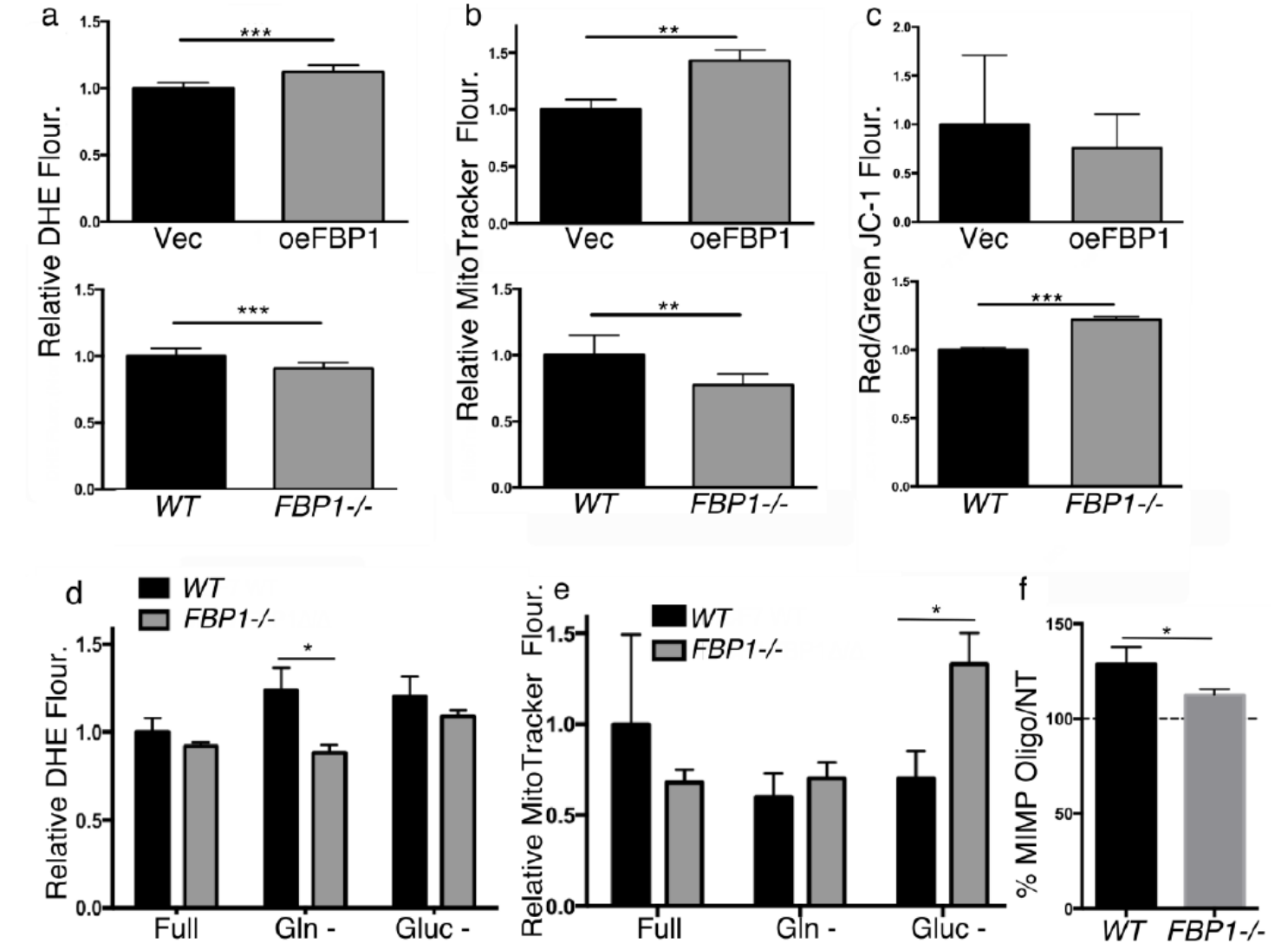

Figure 4

FBP1 increases oxidative stress and mitochondrial biomass in MCF-7 cells. a) ROS accumulation in MCF-7 cells cultivated in full DMEM measured using DHE fluorescence. b) Mitochondrial mass in MCF-7 cells in full DMEM measured using the MitoTracker® Green probe. c) Mitochondrial inner-membrane potential MIMP measured using JC-1 in MCF-7 cells cultivated in full DMEM. In a, b, and c cells were analysed using FACS analysis, the bar-plots feature the fluorescence mean-values ±SD of at least 4 completely

independent replicates of 5000 cells each normalized to the non-treated wild-type or control vector cells. d) ROS accumulation in MCF-7 cells deprived of glucose or glutamine compared to full medium. DHE-labelled cells were analysed using FACS (5000 cells measured). The featured values represent mean ±SD, n=3. e) Mitochondrial biomass in MCF-7 cells deprived of glucose or glutamine compared to full medium. MitoTracker Green labelled cells were measured using FACS, the bar-plots feature the mean-values of at least 3 independent replicates and the error bars represent the standard deviation. f) Relative mitochondrial inner-membrane potential measured following 24 hours of oligomycin (10μM) treatment in MCF-7 cells WT vs FBP1-/-. Depicted are mean-values of three treatments normalized to the non-treated

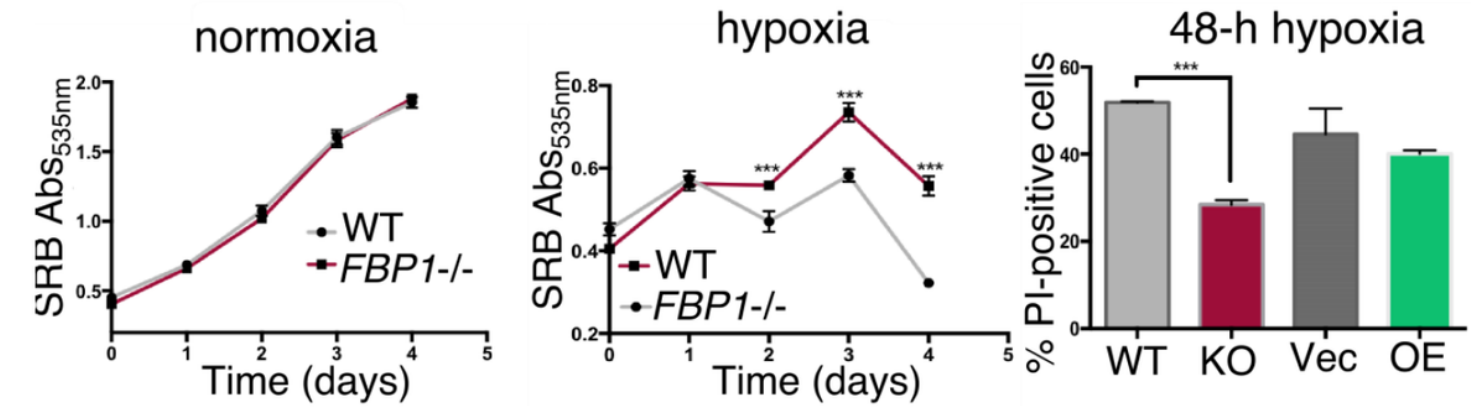

Figure 5

FBP1 knockout improves MCF-7 survival under hypoxic conditions. a&b) SRB proliferation/survival assays of MCF-7 cells FBP1 K.O. vs WT under normoxic and hypoxic (1% oxygen saturation) conditions, respectively. c) Propedium iodide PI staining of dead-cell fractions upon 48-hour of incubation at 1% oxygen saturation. Featured are the percentages of the PI-positive fractions analysed using FACS (5000 cells/sample), mean values±SD, n=3.

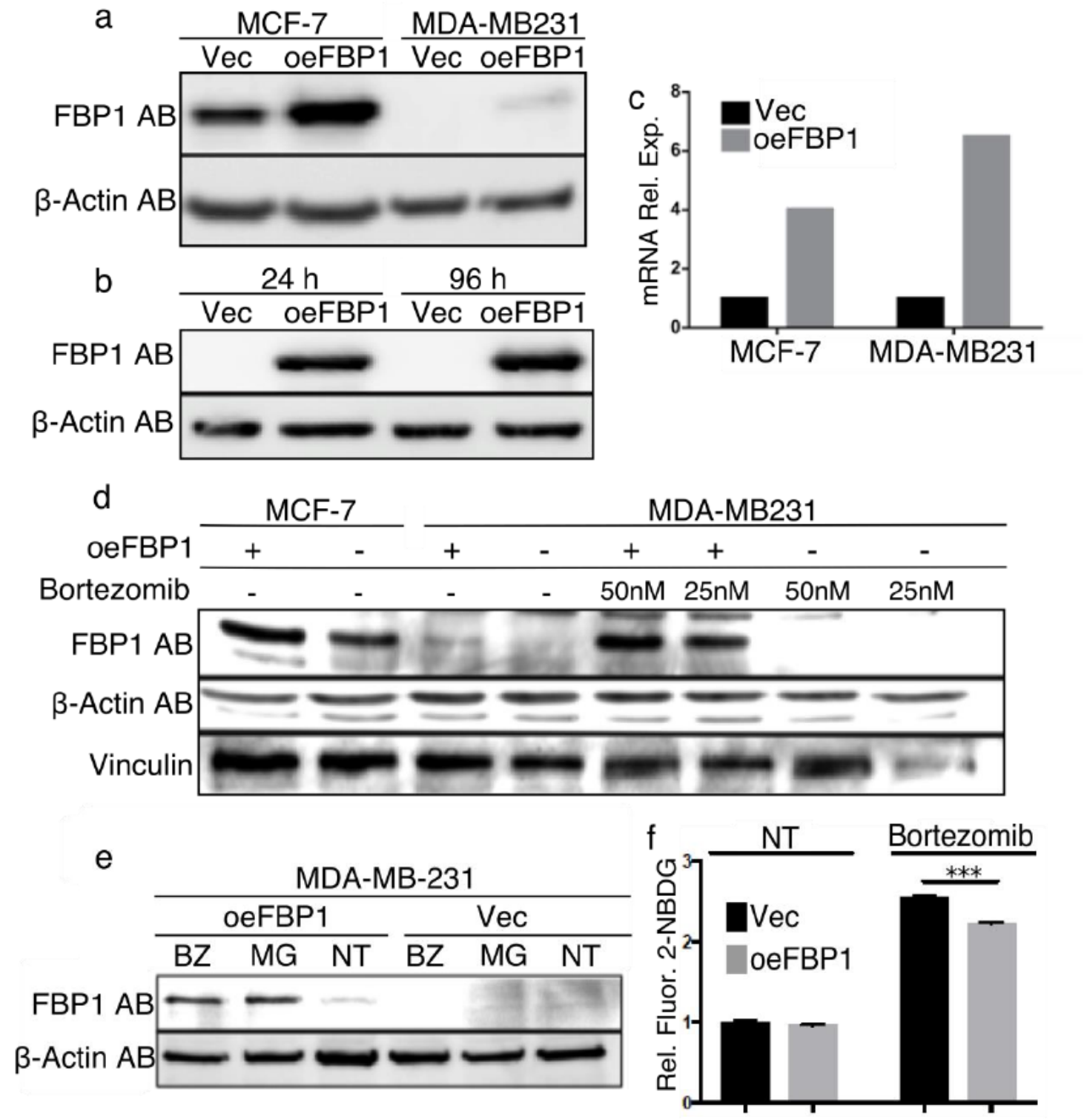

Figure 6

MDA-MB-231 cells degrade the ectopically expressed FBP1. a) Western-blot showing the levels of over-expressed FBP1 in MDA-MB-231 cells compared to those of MCF7 cells. Actin is used as loading control. b) Western-blot showing the expression of FBP1 in MDA-MB-231 following 24h and 96h of transient transfection. Actin was used as a loading control. c) qPCR showing the levels of FBP1 transcripts in MCF-7 and MDA-MB-231 oeFBP1 cells compared to cells carrying the empty vector. Rpl30 was used as a

housekeeping reference gene. d) Western-blot featuring the levels of FBP1 in bortezobmib-treated (48 hours) MDA-MB-231 cells oeFBP1 vs empty vector. Non-treated MCF-7 cells (oeFBP1, vector control) were used as a positive reference for FBP1 expression. Vinculin and actin are used as loading controls. d) Western-blot showing FBP1 levels in MDA-MB-231 cells (oeFBP1 vs vector control) e) Western-blot showing FBP1 levels in MDA-MB-231 cells (oeFBP1, vector control) following 24 hours of bortezomib 50nM (BZ) or MG132 0.5µM (MG) treatments. Actin was used as a loading control. f) Glucose uptake in stably transfected MDA-MB-231 cells (oeFBP1 vs vector). Glucose uptake was compared for non-treated and 24-h 25 nM bortezomib (BZ) treated cells. Glucose uptake was measured using FACS analysis of cells pre-incubated with full DMEM with 2-NBDG. 5000 cells were analysed per replicate, the values represent the mean±SD, n=3.

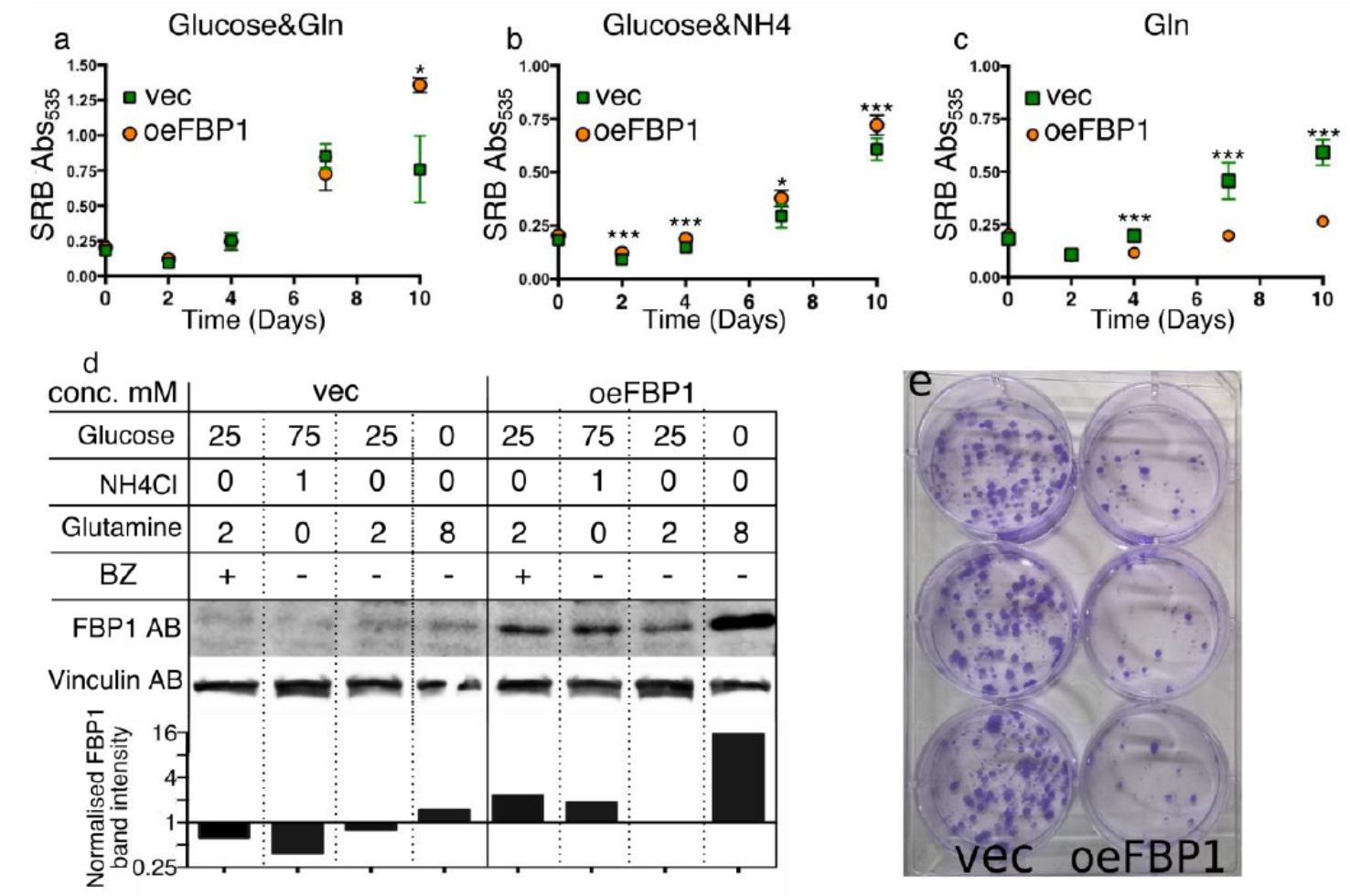

Figure 7

the effects of stable FBP1 expression on MDA-MB-231 cells. A,b&c) SRB proliferation assays of MDA-MB-231 cells oeFBP1 vs vector in various media conditions a) full DMEM with 25mM glucose and 2mM glutamine, b) high glucose 75mM with NH4Cl 1mM as an exclusive nitrogen source c) high glutamine 8mM as the only carbon and nitrogen source. a,b and c) data points represent mean-values ±SD (n=6). Basal ROS accumulation in MDA-MB-231 cells (oeFBP1 vs vector) as measured using FACS analysis of DHE stained cells. 5000 cells of 3 biologically independent replicates were analysed (N=3, error-bar: SD).

d) Western-blot of MDA-MB-231 empty vector and oeFBP1, featuring the regulation of ectopic FBP1 protein levels by variant media conditions. Vinculin expression was used as a loading control. Below is a quantification of FBP1 signal intensities, adjusted to vinculin intensity. Shown are the adjusted FBP1 band-intensity relative to that of the oeFBP1 cells in full DMEM (25mM glucose and 2mM glutamine). e) Colony formation assay of stably transfected MDA-MB-231 cells oeFBP1 vs vector. 200 cells/well were seeded and incubated in full DMEM for two weeks (medium refreshed after 1 week incubation) and then fixed and stained with PFA/crystal violet solution.

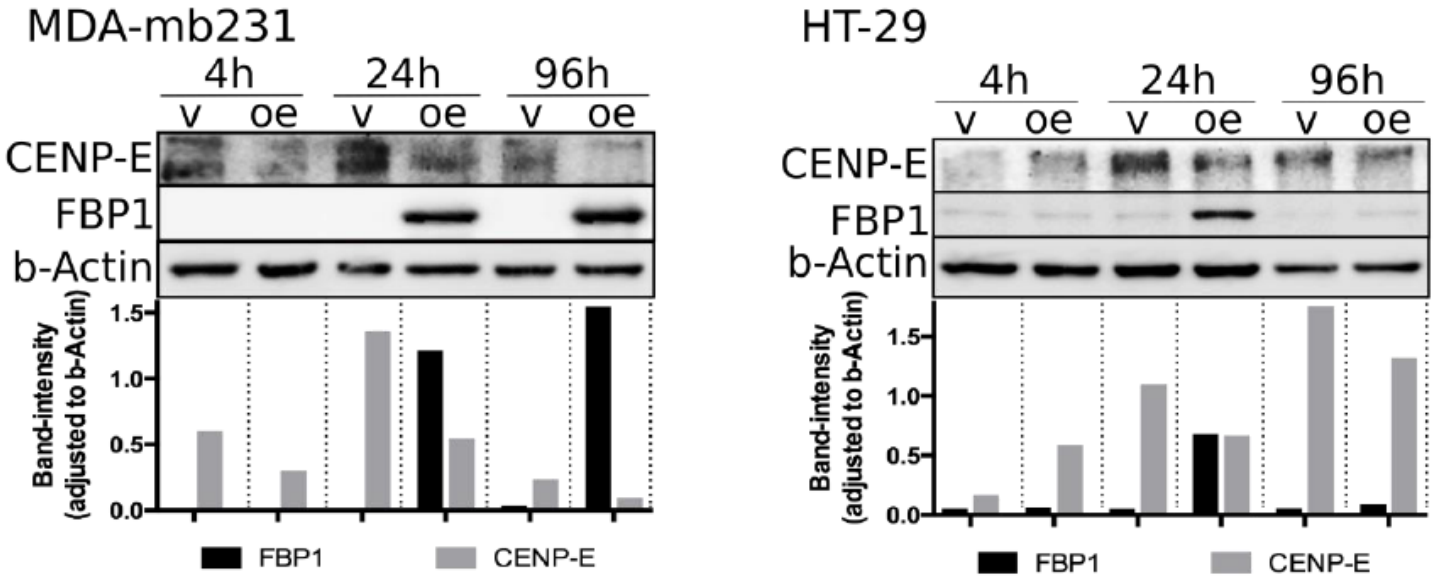

Figure 8

Western-blots showing the levels of transient over-expression of FBP1 4, 24 and 96 hours post-transfection and the concomitant levels of CENP-E. Left: MDA-MB-231, Right: HT-29. (The bar-blots below the western-blots indicate semi-quantification of the FBP1 and CENP-E signals normalized to the respective housekeeping signals).

Supplementary Files

This is a list of supplementary files associated with this preprint. Click to download.

- GraphicalAbstract.png
- SupplementaryMaterials.docx
- Scheme1.png
- Scheme2.png